

Article

Development of a Model for Stormwater Runoff Prediction on Vertical Test Panels Coated with Plaster and Mortar

Pablo Vega-Garcia ^{1,2}, Regina Schwerd ¹, Christian Scherer ¹, Christoph Schwitalla ¹
and Brigitte Helmreich ^{2,*} 

¹ Fraunhofer Institute for Building Physics IBP, Department Environment, Hygiene and Sensor Technology, Fraunhoferstraße 10, 83626 Valley, Germany; pablo.vega.garcia@ibp.fraunhofer.de (P.V.-G.); regina.schwerd@ibp.fraunhofer.de (R.S.); christian.scherer@ibp.fraunhofer.de (C.S.); christoph.schwitalla@ibp.fraunhofer.de (C.S.)

² Technical University of Munich, Chair of Urban Water Systems Engineering, Am Coulombwall 3, 85748 Garching, Germany

* Correspondence: b.helmreich@tum.de; Tel.: +49-89-289-13719

Received: 25 August 2020; Accepted: 14 September 2020; Published: 16 September 2020



Abstract: Leaching outdoor tests (LOT) are commonly used to assess the leaching of substances from construction materials. In this context, the amount of stormwater in contact with the surface material is of special interest for analyzing the runoff loads of substances from building façades. A numerical model was developed in MATLAB on the basis of previous analytical models to calculate the collected stormwater runoff volumes from the vertical test panels (VTP) during LOT. In the model, wind-driven rain (WDR) is considered to be the main mechanism for determining the amount of water impinging on the VTP, so it is a crucial factor in the modeling for the façade runoff. The new model makes it possible to simulate the runoff volumes from VTP that are covered with a wide variety of plaster and mortar. Using the new model, it was possible to relate the VTP runoff volumes obtained during an 18-month sampling period for LOTs performed at the Fraunhofer Institute for Building Physics in Valley, Germany. When comparing the simulation results with the field test accumulated runoffs, the model exhibited a difference of no more than 3.5% for each of the analyzed materials. The simulation results are satisfying, and the paper demonstrates the feasibility of the modelling approach for the runoff assessment of VTP covered with a variety of plaster and mortar.

Keywords: stormwater runoff; wind-driven rain; façade runoff; numerical simulation; plasters

1. Introduction

In the European Community, the evaluation of the environmental properties of building materials has been a high priority for some years. The Construction Products Regulation (CPR) addresses seven basic requirements for buildings [1]. The third requirement covers the area of hygiene, health and environmental protection. According to the latter, construction projects must be designed in such a way that, throughout their entire life cycle, they will not have an exceedingly high environmental impact. Plaster and mortar are mostly used as part of façade external thermal insulation composite systems (ETICS). During the exposure of these products to precipitation and ambient air, the stormwater runoff from the façades dissolves some ingredients from the plaster and mortar. The leached substances can be released into the environment in this way. Since not every substance has an environmentally hazardous potential, the release of substances from construction products in contact with stormwater does not necessarily imply a negative impact on the environment.

Vertical test panels (VTP) (see Figure 1) have been widely used to investigate the leaching of ingredients of building materials, e.g., façade coatings, ETICS, mortars or plasters [2–8]. These panels are commonly used to gain information on the leaching of substances from building products in real weather conditions. However, the evaluation of the leaching behavior of plaster and mortar in the case of a façade in contact with stormwater by using models is not yet possible, as there is no transfer model for reaching conclusions, from the results of leaching tests, on the actual impact of a building product on soil and groundwater.



Figure 1. Vertical test panels used during leaching outdoor tests in Valley, Germany.

During rain events, building ETICS façades become moist due to wind-driven rain (WDR), a horizontal velocity component of the wind that is driven against the windward façade of buildings. WDR is the most important contributor to the moisture load on building façades [2,4,9–13]. Burkhardt [4] first postulated that weather conditions (precipitation, rain intensity, wind speed, wind direction, temperature), façade geometry (height, weight), site characteristics (latitude, altitude) and façade exposure (orientation) are the main influencing factors of the leaching process.

Many studies in recent decades have focused on the prediction of impinging WDR on building façades. These models have focused on predicting the amount of WDR that affects a façade by using semi-empirical formulas [14] and numerical simulations with Computational Fluid Dynamics (CFD). A summary of these methods can be found in Blocken et al. [10]. To approach WDR in a façade, there exist two different methods according to Abuku [15]: (1) The average moisture flux of a façade is supplied by the total mass of all raindrops impinging on the material surface during a defined time interval established by the meteorological input data and (2) the WDR is the sum of individual raindrops impinging on the façade in a spatially and temporally discrete modus. In the CFD model, the airflow patterns were studied using computational fluid dynamics. By using this method, the catch ratios can be calculated by simulating the raindrop trajectories based on the airflow patterns. The raindrop catch ratios are then used to construct distributions for different zones, as a function of the rain intensity and the wind speed. Heat-Air-Moisture (HAM) models have been assessed to take into account the absorption as well as the moisture response of the façade caused by impinging WDR, including drop bouncing and runoff along the surface [16–20]. Liquid film flow models have been largely studied in the past for other disciplines [21–24], but very few investigations have been done coupling them with vertical surfaces and the hygrothermal behaviors of façades [11]. Blocken et al. [9,10] numerically studied the coupling between façade liquid film flows in combination with simplified absorption models like that of Hall and Hoff [25,26]. Simulations typically overestimate the measured moisture content in facades. This may be caused partly by two errors: (1) errors in the difference in absorption and evaporation between an averaged WDR flux and a flux composed of randomly impinging drops, and (2) errors concerning the behavior of the raindrops, as splashing and bouncing may be processes that decrease the availability of water for absorption and laminar flow [20].

The surface runoff that occurs following water saturation of the façade material is of special interest because leaching is controlled by the availability of water in the surface as well as the transport processes within the materials [27]. To model the runoff of the VTP, it is necessary to combine a variety of processes, e.g., WDR impingement in the vertical plane, material absorption, and surface runoff. In this study, the runoff caused by WDR on VTP coated with three different types of plaster and mortar will be simulated. Based on previously developed models, methods and assumptions, the calculation of impinged raindrops in the VTP, as well as the amount of absorbed water and the surface runoff will be assessed. In order to compare the results between the model and the runoff volumes obtained during the field tests, real weather parameters as well as the physical properties of the materials will be used as input parameters.

Over a period of 10 years, the Fraunhofer Institute for Building Physics IBP has carried out systematic and extensive investigations on a large number of formulations of plaster and mortar. A series of field scale tests using vertical test panels comprising various plaster and mortar coatings has been carried out in order to analyze the leaching behavior during real weather conditions as well as in constant physical conditions. The data were used as a basis in the development process of a three-stage model to assess the environmental properties of common plaster and mortar:

- Level 1: Façade runoff model
- Level 2: Model for leaching processes and material transport on façades
- Level 3: Evaluation of the environmental impact by using the leachate forecast for groundwater risk assessment

This study will focus on the “Level 1: Façade runoff model”, in which a runoff numerical simulation model for VTP in MATLAB was developed. The model calculates the water volume that sorbs during the rain event, bounces off the façade, and runs off it or remains on it as a film. The method in this simulation is based on stated assumptions found in previous research papers and existing WDR, absorption, and surface water flow models.

2. Materials and Methods

2.1. Model Parameters

2.1.1. Assumptions and Boundary Conditions

To simulate the amount of stormwater that impinges the VTP, absorbs within the material, and then runs off, a grid was used as the model surface. VTP 0.5 m × 1.0 m in size were therefore divided into elements with sizes of 10 mm × 10 mm. Once the WDR exceeded the absorption rate of the material, water started to accumulate in the form of a film on the studied surface. Water volumes caused by the drops first adhered to the surface and therefore led to more incorporation of drops, rivulets and, finally, a flow film formation. When the water film reached a certain thickness, the gravity forces exceeded the tension forces produced between the impinging water and the material surface. This process allowed the water film to flow down, producing runoff. In order to simulate the runoff in the VTP, each of the elements of the grid consisted of three main layers. The first layer was the (1) cumulative water film thickness (CWFT) (Section “*Cumulative Water Film Thickness (CWFT)*”). This layer defined the point when the cumulated water started to flow downward. If the water film on an element was larger than the CWFT, the water volume that exceeds this film thickness started to flow downward, leaving behind a (2) trace film thickness (Section “*Trace Film Thickness*”). The trace film thickness left behind a trace volume which was equal to the trace water volume multiplied by the size of the grid element. This trace volume then accumulated in the particular element in which the trace volume passed over. The cumulative water film increased depending on the impinging rain amount. The increase in the CWFT was limited by (3) the maximum water thickness (Section “*Maximum Water Thickness*”). This film thickness limited the amount of water that could accumulate in one grid element. If the cumulative element water reached the maximum water thickness, the excess water volume flowed down.

Water rivulets form after water volumes start to run off. Rivulets flow down straight or meander, depending on the flow speed of the rivulet, which is dependent of the flow rate (Section “Flow Speed, Flow Rate and Flow Types”). To simulate individual rivulets in the VTP, the size of the rivulet was proportional to the width of the grid element. The flow path on a grid element was determined by the flow rate and a randomly distributed roughness distribution (Section “Roughness”) that was given to the VTP grid. The approximation of the different flow rates used for selecting whether the rivulet flowed straight or meandered was based on the research of Le Grand-Piteira [28].

The raindrop size distribution was defined by the horizontal rainfall intensity presented by the weather data. This distribution created random raindrops with random diameters in accordance with the mean size presented in the studied area. The random drop impinged a random grid element in every calculation loop defined by a specific time step. Every time a raindrop impinged the VTP, a part thereof splashed off. The remaining volume was partly absorbed, and the rest created a film in the correspondent grid element. If a specific thickness condition was reached, the water flowed down or remained in the grid element as a film waiting for more water to cumulate. The water volume that flowed down was then transported to the grid element beneath. The flow selected the grid element with the lower roughness given by the random roughness distribution. After the volume flowed downward, a part of it left behind a trace volume. If the grid element to which the runoff volume flowed already complied with the condition of the CWFT, the runoff volume continued its way downward, leaving a trace volume in each of the grid elements. The runoff volume stopped in a grid element which had not yet reached the condition of the CWFT and was absorbed or stayed there, depending on the condition of the grid element, until more water cumulated and had the possibility to flow down. In the end, the runoff volume was defined as the runoff volume that flowed all the way down to the bottom of the grid and left the plane. The program ran through every single grid element within each calculation loop and verified the presented conditions. After the program verified the conditions of each of the single grid elements, a new time step defined by the time between each impinging raindrop was created.

2.1.2. Raindrop Size Distribution

The raindrop size distribution used in this study was based on the work described by Best [29]. The model creates a raindrop diameter distribution with a minimum drop diameter ($d0min$) in mm of 0.2 and a maximum drop diameter ($d0max$) in mm of 5.0. A total of 50 raindrop diameter classes (NF) were generated in accordance with the minimum and maximum drop diameter. The class length (CL) was defined by the next equation:

$$CL = \frac{d0max - d0min}{NF} \quad (1)$$

Every class has an average raindrop diameter (d_{avg}) in mm:

$$d_{avg,i} = \frac{(d0_{min,i} + CL)}{2} \quad (2)$$

The class raindrop volumes ($d_{vol,i}$) in mm are created with respect to the average diameters:

$$d_{vol,i} = \frac{4}{3} \cdot \pi \cdot \left(\frac{d_{avg,i}}{2}\right)^3 \quad (3)$$

After obtaining the class raindrop volumes, the Best [29] raindrop distribution is formed. This distribution gives the fraction of the water volume (F_d) in mm³ present in air with diameters equal to $d_{vol,i}$ of a rain event with a specific intensity (R_n) in mm:

$$F_{d,i} = 1 - \exp\left(-\left(\frac{d_{avg,i}}{1.3 \cdot R_n^{0.232}}\right)^{2.25}\right) \quad (4)$$

A raindrop diameter distribution can be constructed by generating a specific quantity of average raindrop diameters for every class. The specific quantity of diameters ($NUM_{F_{d,i}}$) and the fraction of liquid water per unit volume of air (fra_{air}) in mm are calculated with the next equations:

$$NUM_{F_{d,i}} = \frac{F_{d,i} \cdot 10 \cdot fra_{air}}{d_{vol,i}} \quad (5)$$

$$fra_{air} = 67R_n^{0.846} \quad (6)$$

To determine the amount of drops that have to be generated in order to represent a specific event of vertical rain with an intensity equal to R_n , it was necessary to calculate the total water volume of the drops (V_{distr_total}) in mm^3 being generated in that specific rain event with the volume $d_{vol,i}$:

$$V_{distr_total} = NUM_{F_{d,i}} \cdot d_{vol,i} \quad (7)$$

Following the determination of the total water volume of the drops present in a specific rain event, it was necessary to determine how this volume would be distributed on the surface of the grid during the rain event duration (h):

$$V_{in_total} = \frac{R_n}{3600} \cdot h \cdot row \cdot col \cdot DHS \cdot DLS \quad (8)$$

where DHS and DLS are the width and height (mm) of the VTP elements, respectively, and row and col are the number of rows and columns in which the surface was divided.

Lastly, the number of drops that impinge on the surface during a specific rain event ($Raindrop_{num_prosurface}$) with intensity R_n can be calculated with the next equation:

$$Raindrop_{num_prosurface} = \left(\frac{V_{in_total}}{V_{distr_total}} \right) \cdot NUM_{F_{d,i}} \quad (9)$$

The incidence time between each raindrop in seconds d_t was calculated (10). The time between each raindrop determined the time between each calculation loop in the simulation. For each calculation loop, a random raindrop from the raindrop diameter classes was selected. The random raindrop impinged a random grid element.

$$d_t = \frac{T}{Raindrop_{num_prosurface}} \quad (10)$$

2.1.3. Wind-Driven Rain Distribution (CFD Model by Blocken)

The assessment of the WDR intensity in the VTP was based on the catch ratio distribution developed by Blocken [30]. The CFD distribution depends on the wind speed (w_speed), the wind direction ($w_direction$) and the vertical rainfall intensity ($rain_int$).

Several assumptions were made with respect to this model. The first assumption was that the catch ratio of the WDR distribution is independent of the horizontal rainfall intensity. The second assumption was the linear relationship between the magnitude of the catch ratios of the WDR distribution and the wind speed. Therefore, if the wind speed equaled twice the reference wind speed used to calculate the catch ratio in the WDR distribution, the catch ratio was also doubled. The third and last assumption was related to the wind direction. Depending on the wind direction given by the weather file, a WDR distribution was given to the VTP grid. Assuming that all VTP were oriented westward, the relations between the wind direction and the used WDR distribution were as follows:

- [270°–292.5°] distribution derived from 0° wind direction;
- [292.5°–315°] distribution derived from 22.5° wind direction;
- [315°–337.5°] distribution derived from 45° wind direction;

- [337.5°–360°] distribution derived from 67.5° wind direction.

To implement these WDR distributions, each distribution was divided by the amount of grid elements used in the VTP grid. Five hundred grid elements with a specific catch ratio were then determined. This method was used to generate a discrete distribution for each of the four wind directions. To calculate the amount of water impinging ($wall_vol$) the grid elements of the VTP during a rain event in mm, the following equation was implemented:

$$wall_vol(i, j) = (wall_{vol(i,j)} + d_{vol,i}) \cdot WDR_BC(i, j) \cdot \left(1 - \left(\frac{SP}{100}\right)\right) \quad (11)$$

where $d_{vol,i}$ is the raindrop volume that impinged on the grid element, $WDR_BC(i, j)$ is the catch ratio defined by the wind speed and the wind direction, and SP is the splash percentage, which is defined as a constant 30% of the total amount of water impinging on the VTP.

2.1.4. Absorption

The absorption model used for this simulation is that of Hall and Hoff [25]. This model has been used in past runoff models and is tailored to the needs of our simulation [9–12]. The model is composed of two phases. The first describes the absorption of WDR by the VTP surface materials. This absorption requires a constant flux as a boundary condition. This first phase lasts until the saturation of the material, defined by the capillary water absorption coefficient of the material (A), and the impinged water volume ($wall_{vol(i,j)}$) is achieved. The saturation time (t_{sat}), in seconds, is expressed by the following equation:

$$t_{sat} = \frac{A^2}{2 \cdot (wall_{vol(i,j)})^2} \quad (12)$$

If the saturation of the material is not yet reached, the total amount of water that will be absorbed by the VTP (vol_{abs}) will be equal to the total impinged water volume ($wall_{vol(i,j)}$) that can be absorbed per grid element by a specific time (tn). After saturation is reached, the total amount of water that can be absorbed per grid element (vol_{abs}) by a specific time (tn) will be equal to:

$$t_n \leq t_{sat} : vol_{abs} = (wall_{vol(i,j)}) \quad (13)$$

$$t_n > t_{sat} : vol_{abs} = \min(wall_{vol(i,j)}, \frac{A}{2 \cdot \sqrt{tn}} (DHS \cdot DLS)) \quad (14)$$

The initial condition assumed by this model is that the material is dry. This assumption can present a limitation, as mentioned by Blocken [9]. Another limitation of this simplified model is that it does not take material thickness into account. Therefore, the model assumes that, before and after the material is saturated, the moisture from the surface can freely penetrate the material. Since the VTP runoff model focuses on the physical and numerical aspects of stormwater runoff rather than on moisture transfer walls, and our case concerns panels covered with a plaster layer with a maximum thickness of 20 mm (lime cement plaster) rather than walls, the simplified sharp front model by Hall and Hoff [25] fits our purpose.

2.1.5. Runoff

The model includes an assumption that the rainfall intensity is uniformly distributed over the VTP surface. Within each time step, a raindrop impinges on a random grid element in accordance with the raindrop distribution created. A portion of the impinged water splashes, another portion is absorbed and disappears from the surface, and the remaining water flows down the grid element if its water volume is larger than the CWFT and then runs off if the grid element is situated at the bottom of the VTP grid.

Cumulative Water Film Thickness (CWFT)

The CWFT was defined according to Dussan’s [21] force balance equation for droplets in critical static conditions. This derived equation is written in terms of the surface tension force that operates in relation to the contact line of the droplet with the surface and the gravity forces. The CWFT (cw_film_thick), in mm, is described by the following equations:

$$cw_film_thick = \left(\frac{cw_film_vol}{DHS \cdot DLS \cdot row \cdot col} \right) \tag{15}$$

$$cw_film_vol = \left(\frac{\left(\frac{96}{\pi} \right)^{0.5} \cdot \frac{(\cos(\theta_r) - \cos(\theta_a))^{1.5} (1 + \cos(\theta_a))^{0.75} (1 - 1.5(\cos(\theta_a)) + 0.5(\cos^3(\theta_a)))}{(2 + \cos(\theta_a))^{1.5} (1 - \cos(\theta_a))^{2.25}}}{\left(\frac{\rho_w \cdot \left(\frac{g}{1000} \right)}{s_w} \right)^{0.66} \cdot (1000)^3} \right) \tag{16}$$

where cw_film_vol is the volume of water corresponding to the CWFT (mm), θ_r and θ_a are the receding and the advancing contact angles (°) of the material, respectively, ρ_w is the water density (kg/m³), g is the gravitational acceleration (m/s²) and s_w is the surface water tension (N/m).

When the amount of water on a grid element reaches CWFT, the water volume will start to flow down to the grid element below or will run off the VTP if it is situated at the last row of the grid.

Trace Film Thickness

The trace film thickness is the water volume that remains on a grid element after the water flow passes down to the grid element below. Since information is scarce on this topic, a default value of $trace_thick = 0.002$ (mm) was used for each of the different materials.

Maximum Water Thickness

The maximum water thickness (max_film_thick) was defined by the minimum film thickness (δ_{min}) equation for stable films derived by El-Genk [31]. According to El-Genk, this thickness is determined by the minimal total energy equation. The equilibrium surface contact angle can be calculated if the receding (θ_r) and the advancing (θ_a) contact angles are given. To calculate the equilibrium contact angle (θ_0) (°), Tadmor [32] suggested the following equations:

$$\theta_0 = \arccos\left(\frac{r_a \cos \theta_a + r_r \cos \theta_r}{r_a \cdot r_r}\right) \tag{17}$$

With the advancing r_a and receding surface r_r tensions:

$$r_a = \sqrt[3]{\frac{\sin^3 \theta_a}{2 - 3 \cos \theta_a + \cos^3 \theta_a}} \tag{18}$$

$$r_r = \sqrt[3]{\frac{\sin^3 \theta_r}{2 - 3 \cos \theta_r + \cos^3 \theta_r}} \tag{19}$$

El-Genk gives an empirical relation for the dimensionless minimum film thickness:

$$\Delta_{min} = (1 - \cos \theta_0)^{0.22} \tag{20}$$

Finally, the maximum film thickness is given by the next equation:

$$max_film_thick = \frac{\Delta_{min}}{\left(\frac{\rho_w g^2}{15 \mu_l^2 \sigma} \right)^{0.2}} \tag{21}$$

where ρ_w is the water density (kg/m^3), μ is the dynamic viscosity of the water ($\text{N}\cdot\text{s}/\text{m}^2$), and σ is the surface tension of water (N/m) at 20°C .

Flow Speed, Flow Rate and Flow Types

To determine the flow speed of the water that flows during one time step, the parabolic velocity profile of the Nusselt solution [33] was used by simplifying the representation of thin film flow. The use of the Nusselt solution is determined for steady water films, but Blocken [9] proved that the Nusselt solution is plausible for the runoff of water films in vertical planes. The average flow speed of a vertical surface (u) (mm/s^2) is given by the following equation:

$$u = \frac{g \cdot tt^2}{3 \cdot \nu} \quad (22)$$

where g is the gravitational acceleration (mm/s^2), ν is the kinematic viscosity of the water (mm^2/s^2), and tt is the film thickness (mm).

The flow rate between grid elements was defined by the runoff volume. If the cumulative water thickness is complied with, a water volume equal to the runoff volume flowed down to the adjacent grid element beneath. When water volume flowed downward, a part of the water volume remained on the departure grid element (vol_trace). In this regard, the runoff volume was equal to the volume that surpassed the cumulative water thickness minus the trace volume. The runoff volume ($transfer_vol$) divided by the grid element surface represents the transfer film thickness ($transfer_thick$). The assumption was made for the flow rate that the cross-section of the rivulet spreads uniformly over the grid element. From the transfer film thickness and the use of the Nusselt solution, a flow speed (u) can be calculated. The flow rate (Q) in mm^3/s is then given by the following equation:

$$Q = u \cdot transfer_thick \cdot DHS \quad (23)$$

Depending on the flow rate, different flow types may occur. According to Le Grand-Piteira [28], the different flow types and their transition flow rates were “drops” with $Q \leq 200 \text{ mm}^3/\text{s}$, “small straight” with $200 < Q \leq 470 \text{ mm}^3/\text{s}$, “meandering” with $470 < Q \leq 1330 \text{ mm}^3/\text{s}$ and “large straight” with $Q > 1330 \text{ mm}^3/\text{s}$, respectively.

Roughness

Roughness determines the direction of the flow, depending on its flow type. The water volume that flows down as a runoff volume will follow the path with the least resistance. The least resistance grid element below was consequently the one with the lowest roughness. Only the three grid elements beneath the grid element transferring water volume were taken into consideration in determining the flow direction. A change in direction only occurred if the flow rate corresponded to the meandering flow type ($470 < Q \leq 1330$). If the flow rate corresponded to the other flow types, the runoff volume went directly to the grid element below without changing direction.

To define a specific random roughness for every single grid element, a new grid was elaborated (RT). Random roughness coefficients were given to each of the grid elements. This new grid had the first and last column as boundaries. Each of these columns received the highest roughness coefficients in order to serve as an external limitation so that the runoff volume did not go beyond the area size established for the VTP.

Runoff Volume

The runoff volume ($runoff_vol$) was the amount of water that flowed from one grid element to another grid element below. This water volume was the difference between the water volume of the

grid element ($wall_vol(i, j)$) and the water volume that stayed behind after runoff occurred ($trace_vol$). The runoff volume was given by the following equation:

$$runoff_vol = wall_vol(i, j) - cw_film_vol - (trace_{thick} \cdot (DHS \cdot DLS) \cdot 0.1) \quad (24)$$

The runoff volume for each of the grid elements was defined during each time step (d_t). So, if the water volume of the grid element (i, j) was larger than the contact water film volume, a quantity of water equal to the runoff volume flowed away from this grid element and arrived at the element below, which was defined by the flow type and the random roughness determined. If the runoff volume was located in the bottom row of the grid, the water then left the plane and was considered to be runoff ($runoff$).

2.2. Outdoor Tests for Model Validation

The VTP used during the outdoor tests were located in outdoor facilities at the Fraunhofer Institute for Building Physics (IBP) (47°52'30" N, 11°43'41" E) in Valley, Bavaria (Germany). Experimental VTP (each 0.5 m wide, 1 m high) consisting of stainless steel panels were covered by various plasters or mortars (see Figure 1). A detailed description of the sampling site and data analysis are provided in [6,13].

Stormwater runoffs from the VTP were channeled through stainless steel gutters into canisters. Forty-nine rain events were collected and analyzed over a monitoring period of 18 months. After each single rain event, the total volume of the runoff corresponding to each VTP was measured by weighing. A weather station (Davis Vantage Pro) was installed on site during the monitoring period. The weather station used was capable of recording wind speeds up to 322 km/h, temperatures between -40 °C and 65 °C, and precipitation height in 0.2 mm increments. Precipitation heights (vertical rain), temperature, wind speed and wind direction were recorded every 5 min. The recorded weather data of the study site were used as input data in the VTP runoff model.

In Valley, there are approximately 180 rainy days per year. The monthly precipitation during the test period, from October 2013 to March 2015, ranged from 8.7 mm (L/m^2) in December 2013 to 224 mm in August of 2014. Detailed information about the daily precipitation during the sampling period and the runoff sampling dates are provided in [13]. During the 526-day observation period, precipitation events with more than 0.1 mm of rain occurred for 255 days. The strongest rain event occurred on August 2, 2014, reaching 60.4 mm. The lowest temperature recorded during the study period was -16.1 °C (29 December 2014). The highest temperature of 32.1 °C was measured on 19 June 2014. The wind at the sampling site came mainly from the westerly and southwesterly directions [13]. The highest daily mean wind speed observation was 66 km/h on 31 March 2015. During this day, the gusts reached a maximum speed of 98 km/h [13].

The weather file was composed of an Excel file. Each of the columns of the file represented a measurement in 5-min intervals of rainfall intensity ($rain_int$) in mm/h, wind speed (w_speed) in m/s, wind direction ($w_direction$) in degrees, and temperature ($temp$) in °C. For each of the parameters, a column matrix was introduced into MATLAB, where each row represented the magnitude of the 5-min measurement.

To convert these micro-meteorological boundary conditions into impinging rain along the VTP, the WDR catch ratio distributions by Blocken [30] were used, as stated in Section 2.1.3.

2.3. Model Input Parameters

A combination of parameters was used in order to illustrate the comparison between the different input parameters of the model. The VTP had a surface of 1.0 m by 0.5 m. It was assumed that a rainfall intensity of 2.5 mm/h would impinge the VTP. The total duration of the rain event was set to 1, 2, 3 and 5 h. The wind direction was constantly perpendicular to the VTP (0°). A constant splash percentage of 30% was maintained during the simulation, and the absorption coefficient was set to

$0.01 \text{ mm}^3/\text{mm}^2\text{s}^{0.5}$. The ambient temperature was fixed to $10 \text{ }^\circ\text{C}$. The absorption coefficient values used in the simulation were taken out of the German standard norm DIN EN 998-1 [34].

2.4. Boundary Conditions for Runoff Simulation

A 315-day simulation run was conducted on the basis of weather data measured during the VTP runoff outdoor tests. The data were available on a 5-min basis, which is a permissible time step for WDR measurements in accordance with Blocken [35]. The daily sum of the 5-min intervals where the rain event occurred was equal to the effective daily rain duration. At the start of every simulation cycle, the VTP was in balance with the outdoor environment. The effects of previous moisture loads and drying periods were neglected due to this initial condition. The moisture fluxes on the VTP were only dependent on the impinged WDR. Due to the neglected previous processes and high relative humidity (near 100%) during rain events, evaporation processes were not considered.

The simulated runoffs were added up in order to obtain daily cumulative results. These results were then compared with the actual obtained cumulative runoffs from the outdoor tests in order to prove the veracity and accuracy of the model.

3. Results

The runoff was calculated using the established absorption model and the WDR distribution assessment model of Blocken [30]. The flow speed and the film thickness were analyzed and compared to the solutions of Beijer and Nusselt. Finally, the results were compared with existing runoff volumes obtained over an 18-month VTP outdoor testing period.

3.1. Wind-Driven Rain Distribution

In the CFD Model by Blocken [30], the WDR load in the VTP was determined by the multiplication of catch ratios with the rainfall intensity. In Figure 2, the WDR distribution for 0° , which was used for the previously specified rain event, can be seen. The figure shows that the magnitude of impinged water volume varies according to the exposure time of the VTP to the rain event. The upper edges of the VTP received the highest amount of WDR, while the lower part received the least amount of WDR.

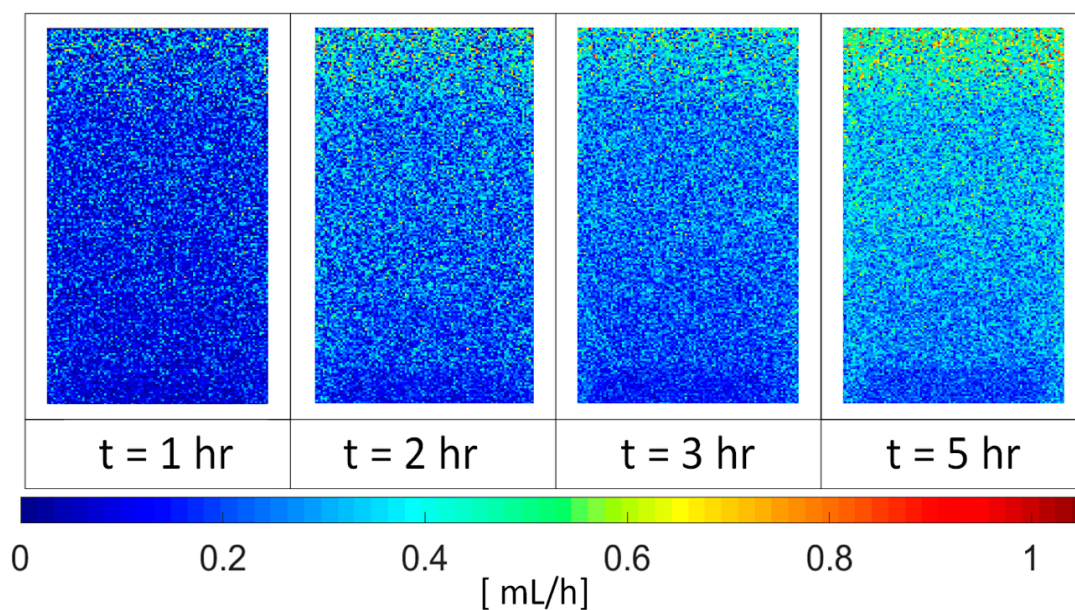


Figure 2. Impinged water volumes on vertical test panels (VTP) for time $t = 1 \text{ h}$, 2 h , 3 h and 5 h using the wind-driven rain Computational Fluid Dynamics (CFD) model by Blocken [30].

For the VTP that was exposed for $t = 5$ h, some elements in the upper edges received up to 0.8 mL and 1.2 mL of water in comparison with the VTP exposed to $t = 1$ h, which only received up to 0.4 mL during the rain event. The cumulative WDR received by the VTP for the surface exposed to $t = 1$ h was 1.3 L, for $t = 2$ h 2.5 L, for $t = 3$ h 3.8 L, and for $t = 5$ h 6.4 L.

3.2. Amount of Absorbed Water

The Hall and Hoff [25] model was implemented to include the absorption parameters in the model. To investigate the amount of absorbed water, the same standard parameters as those described in Section 2.3 were used in conjunction with the CFD model by Blocken. The total height of the VTP was assumed to have the same capillary water absorption coefficient.

For the VTP exposed to $t = 2$ h, a total absorption of 1.05 L was found. After $t = 4284$ s, the material was fully water saturated, and the water started to accumulate on the surface. The total amount of WDR available on the plane during the rest of the rain event was 0.87 L. This water volume was later available for runoff. The observed absorption and accumulated water volume in the material can be seen in Figure 3. The sorption capacity of the material led to a quick saturation of the surface and the building of runoff. If the water volume in the material was not taken into account, an underestimation of almost 45% of the moisture content after 1 h took place on the VTP. These results are similar to those presented by Van den Brande [12].

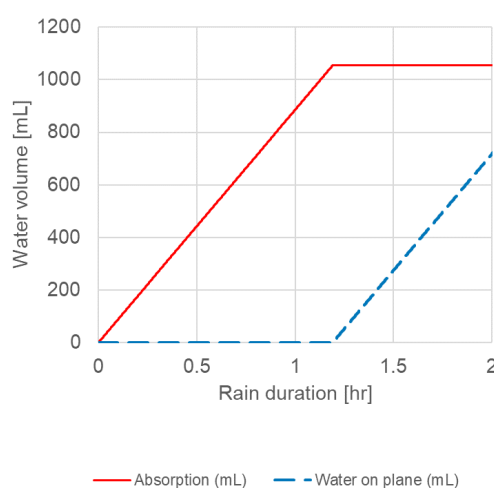


Figure 3. Accumulated water volume on the material and accumulated absorption during a defined standard rain event when implementing the Hall and Hoff [25] model.

3.3. Water Film Thickness

In Table 1 the CWFT, the absorption coefficient and the results for a rain event with a duration of 2 h are depicted for three façade materials. The rain event standard parameters presented in Section 2.3 were used for this simulation.

Table 1. Cumulative water film thickness (CWFT) simulation results for the three different plasters after 7200 s (2 h). Absorption coefficient values according to DIN EN 998-1 [34] and contact angles according to [36].

Material	CWFT [mm]	Equilibrium Contact Angle [°]	Capillary Absorption Coefficient [$\text{mm}^3/(\text{mm}^2 \cdot \text{min}^{0.5})$]	Absorption Volume [mL]	Surface Cumulative Volume [mL]	Runoff Volume [mL]
Facing masonry mortar	0.0204	83.8	0.16	210	1563	1539
Lime cement render	0.0212	82.9	0.39	1305	469	431
Scrap render	0.0215	83.1	0.31	836	939	871

These absorption coefficient values are commonly used in the plaster and mortar industry as standard values. In accordance with the contact angles given by Steffgen [36], mineral-bound plasters have angles of $<90^\circ$. The CWFT is mainly influenced by the contact angles of the material, but this influence can be neglected because the plasters tested were mainly composed of mineral-bound materials and compositions very similar to those in Table 1. As seen in Table 1, the main parameter having an influence on the runoff volume was the absorption coefficient of the material. This parameter limits the amount of water that cumulates on the façade surface after a certain time duration of a rain event. The water film thickness varied with time (Figure 4). Film formation only started after the material's absorption boundary condition was complied with. For the lime cement render, this film thickness was formed after 1 h of receiving WDR impingement. Meanwhile, regarding the other two materials, this film was formed within the first hour of the rain event. The reason for this was that the lime cement render has a higher absorption coefficient ($A = 0.05 \text{ mm}^3/\text{mm}^2\text{s}^{0.5}$) than the other two materials, thus absorbing more water. As a result, it needed more time to start forming a surface water film. The maximum film thicknesses during the rain event were 0.22 mm, 0.19 mm, and 0.23 mm for the facing masonry mortar, lime cement render, and scrap render, respectively. After applying the absorption boundary condition, the film thickness continued to grow, and the water travelled down the VTP. This behavior could also be observed in the flow rate figures when comparing the first hour of the facing masonry mortar with the plasters. Runoff started within the first hour for the facing masonry mortar, meaning that the wall absorbed enough water before complying with the absorption boundary condition and, subsequently, forming a water film thickness thick enough to start the transportation of the water down the surface of the VTP. This behavior was not evident for the other two materials, meaning that no runoff was present within the first hour. When runoff occurred, the flow rate at the center and bottom of the VTP was constant, meaning that most of the water impinging on the upper side of the VTP tended to flow downward, thus causing higher flow rates in the center and bottom part of the VTP. This effect was observed for all three materials. Higher flow rates were achieved in the facing masonry mortar (0.78 L/m), which tended to accumulate higher amounts of water volume on its surface due to a lower capillary absorption coefficient. With respect to the lime cement render and the scrap render, no flow rate resulted within the first hour of the rain event, meaning that there was not enough water on the surface of the VTP to start the runoff. This behavior was directly related to the formation of the water film thickness and the absorption capacity of the material.

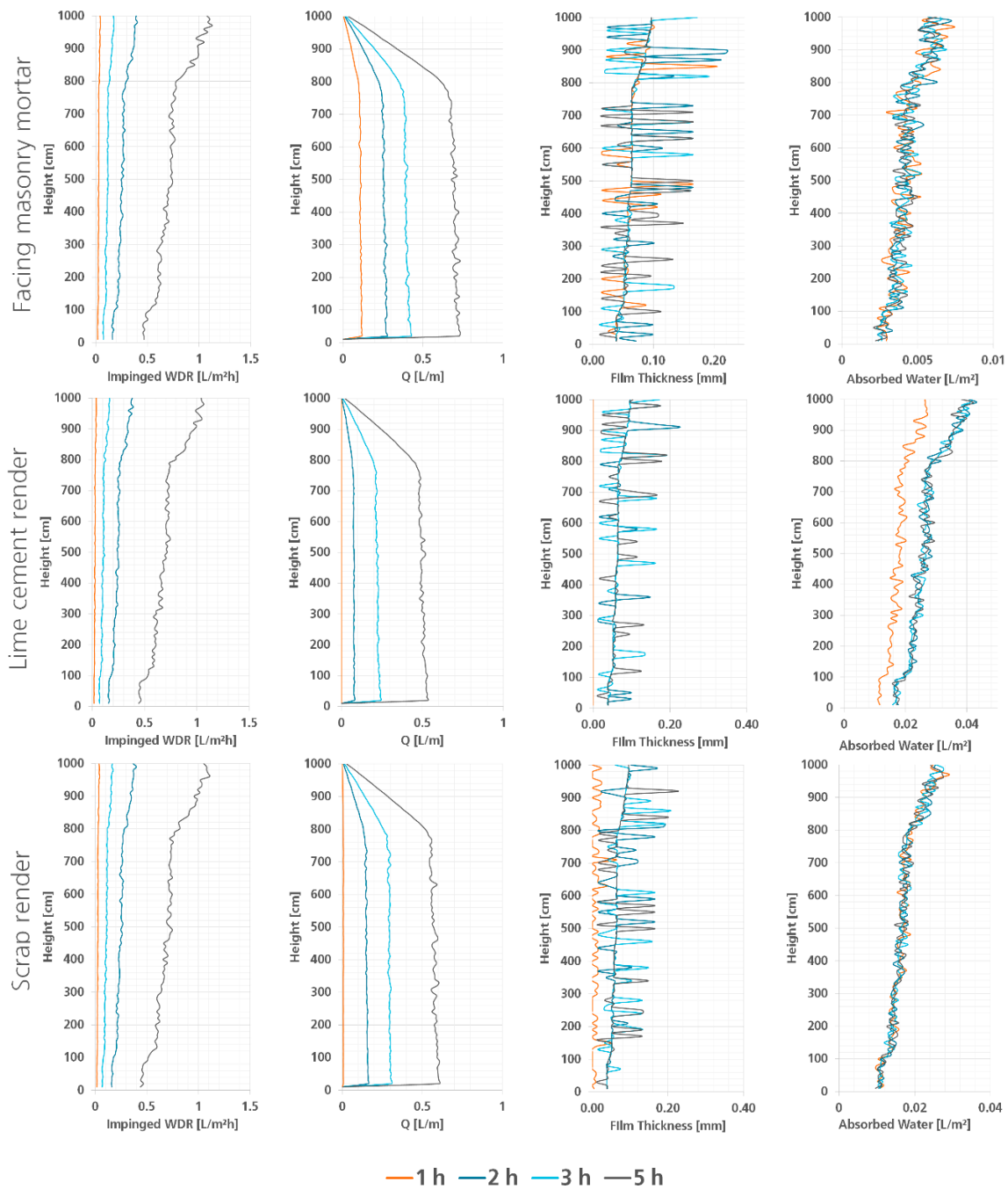


Figure 4. Impinged wind-driven rain during 1 h, 2 h, 3 h and 5 h intervals. Corresponding numerical results for the 1 m high VTP at different time steps and different materials, for flow rate, film thickness and total absorbed water.

3.4. Runoff Volume (Simulation and Model Validation with Outdoor Tests)

To demonstrate the possibilities of the VTP runoff model and to evaluate the results provided, actual rain events were simulated on VTP covered by three different types of plaster and mortar. The characteristics of the materials are shown in Table 1. The runoff results were then compared with those obtained during the outdoor tests.

A period of 315 days was simulated using the VTP runoff model. For the facing masonry mortar, the cumulative runoff volume obtained in the field tests after 315 days was 65.3 L, whereas the VTP runoff model obtained 63.1 L as a cumulative runoff result for this same material. The outdoor test

cumulative runoff volumes for the lime cement render and the scrap render were 28.6 L and 45.4 L, respectively. The results obtained by the model for the previously mentioned materials were 29.5 L and 46.0 L. The difference between the results obtained in the field tests and the results provided by the model at the end of the simulation was less than 3.5%. The results of the simulation vs. the outdoor test cumulative runoff volumes for the three materials are depicted in Figure 5.

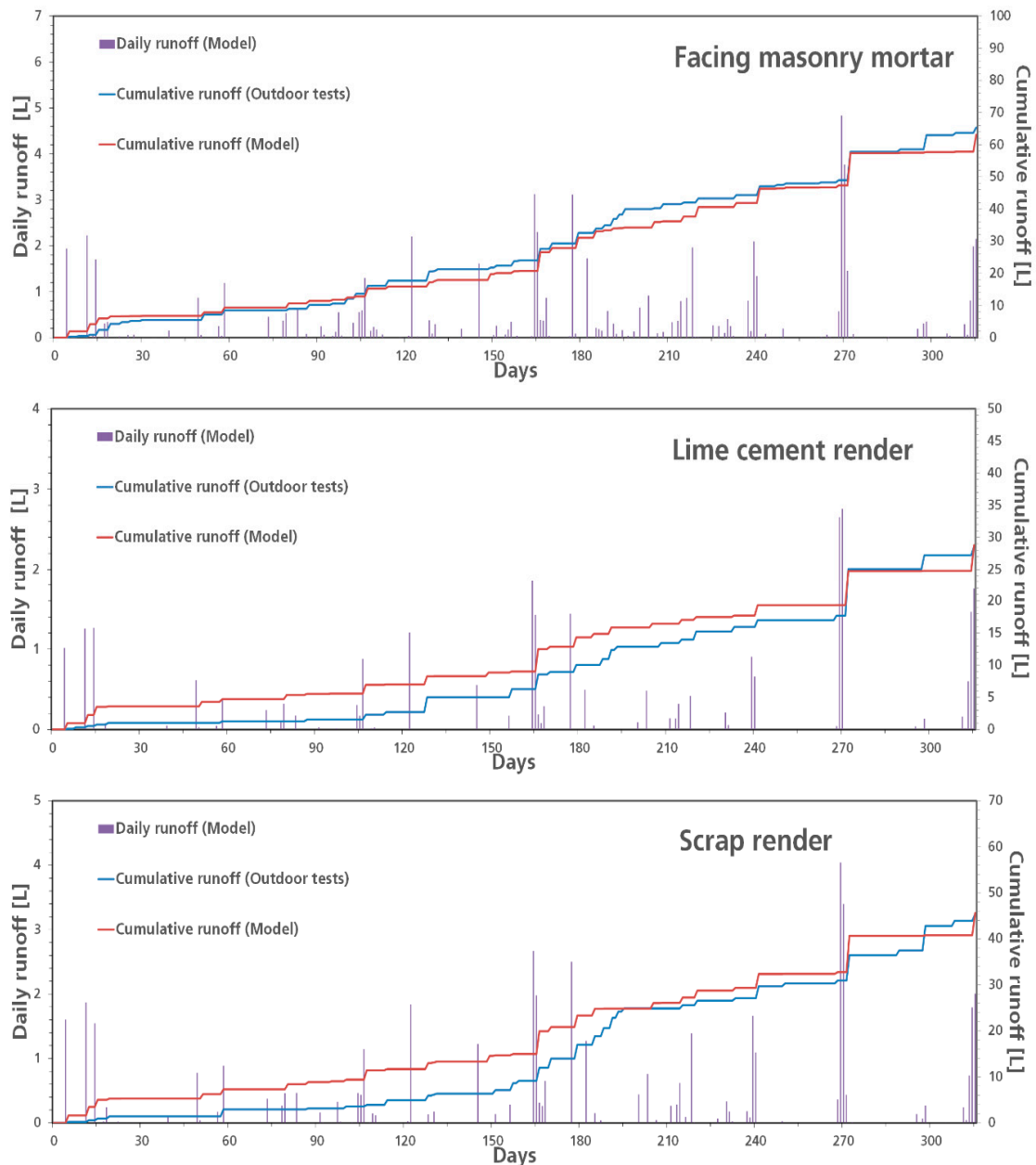


Figure 5. VTP daily-simulated runoff and cumulative simulated/actual runoff for facing masonry mortar (up), lime cement render (middle) and scrap renders (down).

The day with the highest collected runoff for the three VTP was 24 October 2014 (Day 268). The weather measurements indicated that, the day before the runoff was collected from the canisters, 38 mm of rain fell during a time span of 16 h with average wind speeds of 5.5 km/h, coming mainly from the southwest. During this day, total volumes of 8.8 L, 7.3 L and 5.5 L were collected for the facing masonry mortar, the lime cement render and the scrap render, respectively. The model also simulated the highest runoff on this day for the three VTP. The simulated runoff during this day for the

facing masonry mortar was 10.1 L. For the lime cement render and the scrap render, simulated runoffs of 8.4 L and 7.9 L were obtained, respectively. The difference between the collected runoff and the modelled runoff can be attributed to several factors. Due to the intensity of the rain event and the time it lasted, these factors may have varied more. One of the possible reasons for the variation in the runoff might be that the amount of water that splashed off the VTP was more than that stipulated in the model (30%). It is likely that the existence of a greater number of drops impinging the VTP meant that they splashed due to the speed at which they were directed to the VTP surface. Another possible reason for this over-estimation is that the model does not include evaporation processes. Although the relative humidity during rain events like this type approaches 100%, it is possible that some quantity of water evaporated during and after the rain event.

The model simulated a total of 126 days when the VTP presented runoff on the facing masonry mortar, 53 days of which the runoff was below 100 mL, with 40 days between 100 mL and 500 mL, and 33 days over 500 mL. For the lime cement render, runoff was presented in 67 days, 33 of which presented a runoff below 100 mL, 18 days between 100 mL and 500 mL, and just 16 days over 500 mL. Finally, the scrap render presented 93 days with runoff, of which 40 days presented a runoff below 100 mL, 31 days between 100 mL and 500 mL, and 22 days over 500 mL. The lime cement render presented less runoff events than the facing masonry mortar and the scrap render. This behavior was mainly dependent on the capillary absorption capacity of the material. Despite the fact that the least rainy days were recorded during the first days of testing (the first 100 days), the model yielded runoff results on some days that were not obtained in the outdoor test samples. This behavior is shown in Figure 5, in which the first cumulative daily runoffs given by the model for the lime cement render and the scrap render were not observable in the outdoor test results. One reason for this might be that the VTP absorbed more water than predicted by the model. Another reason might be that, during these rain events, the relative humidity of the field was not very high due to the low rain intensity and higher evaporation on the surface of the VTP. This last process was not represented in the facing masonry mortar results. Often, these effects were not visible during the rain events with greater intensity because the amount of water absorbed was very low in comparison with all of the impinged WDR. It is also possible that, during the effects of heavy rain, the relative humidity of the area was very high, and the evaporation process may have been neglected.

3.5. Advantages and Limitation of the Model

Given the results obtained by the simulations, the advantages and limitations of the model can be described. For the most part, the limitations of the model go hand in hand with the constant variation in the weather data in reality vs. the assumptions made in the model (e.g., VTP surface temperature at 20 °C). It is possible that these types of assumptions limited or influenced the calculation of runoff volumes and gave underestimated or overestimated results for certain simulated rain events. One example of this can be seen in Figure 5, in which, during the first 100 days, the model showed runoff in some of the events although no runoff volumes were collected in the field. As also observed by Blocken [9], many of the limitations in the VTP model are caused by the adopted simplifications, e.g., the use of the Nusselt solution to determine the flow film while not taking into account wave behavior, especially in strong rain events. Simulated values in certain rain events can be overestimated because drying or evaporation were not included in the model. For very weak rain events, these processes can have a very important impact and can be noticeable in the simulation of the first rain events, which were characterized by very weak precipitation. Another limitation of the model was that the method used to give roughness to the VTP is the same for all three types of materials. The materials used in the field experiments showed physical differences in their surfaces, depending on the grain size of the mixture. One example of this is the lime cement render, which is a material with grains larger than plaster (max. 2 mm grain), making its surface less smooth. This physical characteristic of the material may play an important role in stream formation and could complicate the runoff patterns.

A method for correctly defining the difference between the roughness of varying materials should be evaluated in future investigations.

Despite the limitations caused by model uncertainties, the results obtained by the model and the results obtained in field tests (see Figure 5) exhibited a difference of no more than 3.5% of the accumulated runoff volumes for each of the analyzed materials. Using the runoff model, it is possible to investigate and to reproduce the runoff response of a VTP characterized by a specific plaster or mortar for a defined location and period of time, and obtain a good approximation of the amount of runoff that each material will have. The WDR load that is received by the VTP can be calculated on the basis of inputted weather parameters given by a weather dataset of the studied region. Depending on the weather conditions, an estimation of the runoff volumes can be determined. Additionally, the model can be adjusted to different materials. Given the use of some specific parameters like the capillary absorption coefficient and the contact angles, it is possible to differentiate the runoff behavior on the surfaces of various material types. In this way, the model makes it possible to predict the amount of runoff water volume from VTP results without needing to obtain samples of larger façades. These runoff results could help predict the runoff and leaching behavior of larger façades without having to reproduce them in the field in order to validate them.

4. Conclusions

Our runoff model is “Level 1” of a three-stage model. In the model described, existing modeling methods were adapted for the prediction and evaluation of rainwater runoff from VTP. Due to the incorporation of real weather data, it was possible to simulate a series of rain events over a period of 315 days. The advantage of having a complete and detailed experimental dataset made it possible to validate the accuracy of the model by comparing the simulated results with those collected in the field. Despite the limitations of the model, caused by uncertainties, the difference between the simulated and the field data was no more than 3.5% of the accumulated runoff volumes for the analyzed materials.

The presented runoff model makes it possible to investigate and reproduce the runoff response of VTP characterized by a specific plaster or mortar for a defined location and period and obtain a good approximation of the amount of runoff for different materials. First, the rain loads can be calculated and visualized with the aid of the simulation program; secondly, the total absorption of the material can be estimated at any time in accordance with the used absorption model, and, finally, the runoff volume and water flow rate on the VTP can be determined. The moisture content of the VTP is largely dependent on the supplied WDR and the material characteristics. We observed that higher runoff volumes and flow rates are more likely to appear on materials with a lower capillary absorption capacity.

Flow rates and runoff volumes are of significant importance and can be used for the prediction of leaching substances (“Level 2”). The development and evaluation of the models of “Level 2” and “Level 3” will be the subject of further publications.

Author Contributions: P.V.-G.: writing—original draft, validation, formal analysis, methodology, conceptualization, data curation, investigation. R.S.: conceptualization, supervision, writing—review and editing, project administration. C.S. (Christian Scherer): supervision, funding acquisition, writing—review and editing. C.S. (Christoph Schwitalla): project administration. B.H.: supervision, writing—review and editing. All authors have read and agreed to the published version of the manuscript.

Funding: This research received no external funding.

Acknowledgments: This project was kindly supported by the Association for Insulation Systems, Plaster and Mortar, Germany (VDPM) and several German manufacturers of building products. This work was supported by the German Research Foundation (DFG) and the Technical University of Munich (TUM) in the framework of the Open Access Publishing Program.

Conflicts of Interest: The authors declare no conflict of interest.

References

1. EUR-Lex. (2011, March). Regulation (EU) No 305/2011 of the European Parliament and of the Council of 9 March 2011 Laying Down Harmonized Conditions for the Marketing of Construction Products and Repealing Council Directive 89/106/EEC Text with EEA Relevance. Available online: <https://eur-lex.europa.eu/legal-content/EN/TXT/?uri=celex%3A32011R0305> (accessed on 1 June 2020).
2. Bester, K.; Vollertsen, J.; Bollmann, U.E. *Water Driven Leaching of Biocides from Paints and Renders*; Pesticide Research No. 156; Danish Ministry of the Environment: Copenhagen, Denmark, 2014; ISBN 978-87-93178-11-3.
3. Bollmann, U.; Vollertsen, J.; Carmeliet, J.; Bester, K. Dynamics of biocide emissions from buildings in a suburban stormwater catchment—concentrations, mass loads and emission processes. *Water Res.* **2014**, *56*, 66–67. [[CrossRef](#)] [[PubMed](#)]
4. Burkhardt, M.; Zuleeg, S.; Vonbank, R.; Bester, K.; Carmeliet, J.; Boller, M.; Wangler, T. Leaching of biocides from facades under natural weather conditions. *Environ. Sci. Technol.* **2012**, *46*, 5497–5503. [[CrossRef](#)]
5. Hensen, B.; Lange, J.; Jackisch, N.; Zieger, F.; Olsson, O.; Kümmerer, K. Entry of biocides and their transformation products into groundwater via urban stormwater infiltration systems. *Water Res.* **2018**, *144*, 413–423. [[CrossRef](#)]
6. Schwerd, R.; Scherer, C.; Schwitalla, C. Umwelteigenschaften mineralischer Werkmörtel und pastöser Produkte (Environmental properties of mineral mortar). *Vom Wasser* **2017**, *115*, 40–41.
7. Schwerd, R. *Verweilverhalten Biozider Wirkstoffe in Aussenbeschichtungen Im mehrjährigen Freilandversuch (Residence Behavior of Biocidal Active Substances in External Coatings in Multi-Year Field Trials)*; Forschungsergebnisse aus der Bauphysik; Fraunhofer Verlag: Stuttgart, Germany, 2011; ISBN 978-3-8396-0289-8.
8. Schwerd, R.; Scherer, C.; Breuer, K. Wirkstoff-Restgehalte verkapselter und freier Biozide in hydrophoben Fassadenbeschichtungen (Remaining active substance content of encapsulated and free biocides in hydrophobic facade coatings). *Bauphysik* **2015**, *37*, 308–314. [[CrossRef](#)]
9. Blocken, B.; Carmeliet, J. A simplified numerical model for rainwater runoff on building facades: Possibilities and limitations. *Build. Environ.* **2012**, *53*, 59–73. [[CrossRef](#)]
10. Blocken, B.; Derome, D.; Carmeliet, J. Rainwater runoff from building facades: A review. *Build. Environ.* **2013**, *60*. [[CrossRef](#)]
11. Van den Brande, T.; Teblich, L.; Blocken, B.; Roels, S. Influence of facade materials on runoff due to wind-driven rain. In Proceedings of the 5th International Building Physics Conference (IBPC), Kyoto, Japan, 28–31 May 2012; pp. 149–154.
12. Van den Brande, T.; Teblich, L.; Blocken, B.; Roels, S. Rainwater runoff from porous building facades: Implementation and application of a first-order runoff model coupled to a HAM model. *Build. Environ.* **2013**. [[CrossRef](#)]
13. Vega-Garcia, P.; Schwerd, R.; Scherer, C.; Schwitalla, C.; Johann, S.; Rommel, S.H.; Helmreich, B. Influence of façade orientation on the leaching of biocides from building façades covered with mortars and plasters. *Sci. Total Environ.* **2020**, *734*, 139465. [[CrossRef](#)]
14. ISO. (2009, March). ISO 15927-3:2009 Hygrothermal performance of buildings—Calculation and presentation of climatic data—Part 3: Calculation of a driving rain index for vertical surfaces from hourly wind and rain data. Available online: <https://www.iso.org/standard/4428.html> (accessed on 1 August 2020).
15. Abuku, M.; Blocken, B.; Roels, S. Moisture response of building facades to wind driven rain: Field measurements compared with numerical simulations. *J. Wind. Eng. Ind. Aerodyn.* **2009**, *97*, 197–207. [[CrossRef](#)]
16. Künzel, H. Simultaneous Heat and Moisture Transport in Building Components. One- and Two-Dimensional Calculation Using Simple Parameters. Ph.D. Thesis, Fraunhofer IRB, Stuttgart, Germany, 1995.
17. Künzel, H.; Kiessl, K. Calculation of heat and moisture transfer in exposed building components. *Int. J. Heat Mass Transf.* **1996**, *40*, 159–167. [[CrossRef](#)]
18. Blocken, B.; Roels, S.; Carmeliet, J. A combined CFDHAM approach for wind-driven rain on building facades. *J. Wind. Eng. Ind. Aerodyn.* **2007**, *95*, 585–607. [[CrossRef](#)]
19. Janssen, H.; Blocken, B.; Carmeliet, J. Conservative modeling of the moisture and heat transfer in building components under atmospheric excitation. *Int. J. Heat Mass Transf.* **2007**, *50*, 1128–1140. [[CrossRef](#)]
20. Abuku, M.; Janssen, H.; Poesen, J.; Roels, S. Impact, absorption and evaporation of raindrops on building facades. *Build. Environ.* **2009**, *44*, 113–124. [[CrossRef](#)]

21. Dussan, V.E.B.; Chow, R. On the ability of drops or bubbles to stick to nonhorizontal surfaces of solids. *J. Fluid Mech.* **1983**, *137*, 1–29. [[CrossRef](#)]
22. Ruyer-Quil, C.; Manneville, P. Modeling film flows down inclined planes. *Eur. Phys. J. B* **1998**, *6*, 277–292. [[CrossRef](#)]
23. Ruyer-Quil, C.; Manneville, P. Improved modeling of flows down inclined planes. *Eur. Phys. J. B* **2000**, *15*, 357–369. [[CrossRef](#)]
24. Savva, N.; Kalliadasis, S. Dynamics of moving contact lines: A comparison between slip and precursor film models. *EPL (Europhys. Lett.)* **2011**, *94*, 1–6. [[CrossRef](#)]
25. Hall, C.; Hoff, W. *Water Transport in Brick, Stone and Concrete*; Spon Press: London, UK; New York, NY, USA, 2002.
26. Hall, C.; Hoff, W. Water Movement in Porous Building: Evaporation and Drying in brick and block materials. *Build. Environ.* **1984**, *19*, 13–20. [[CrossRef](#)]
27. Schoknecht, U.; Mathies, H.; Wegener, R. Biocide leaching during field experiments on treated articles. *Environ. Sci. Eur.* **2016**, *28*, 2–10. [[CrossRef](#)]
28. Le Grand-Piteira, N.; Daerr, A.; Limat, L. Meandering Rivulets on a plan: A simple balance between inertia and capillarity. *Phys. Rev. Lett.* **2006**, *96*, 254503. [[CrossRef](#)]
29. Best, A. The size distribution of raindrops. *Q. J. R. Meteorol. Soc.* **1950**, *76*, 16–36. [[CrossRef](#)]
30. Blocken, B.; Carmeliet, J. On the validity of the cosine projection in wind-driven rain calculations on buildings. *Build. Environ.* **2006**, *41*, 1182–1189. [[CrossRef](#)]
31. El-Genk, M.; Saber, H. Minimum film thickness of a flowing down liquid film on a vertical surface. *Int. J. Heat Mass Transf.* **2001**, *44*, 2809–2825. [[CrossRef](#)]
32. Tadmor, R. Line Energy and the Relation between Advancing, Receding and Young contact angles. *Langmuir* **2004**, *20*, 7659–7664. [[CrossRef](#)] [[PubMed](#)]
33. Nusselt, W. Die Oberflächenkondensation des Wasserdampfes. *Z. Ver. Dtsch. Ing.* **1916**, *60*, 569–575.
34. DIN. (2017, February). DIN EN 998-1:2017-02 Festlegungen für Mörtel im Mauerwerksbau—Teil 1: Putzmörtel. Available online: <https://www.din.de/de/mitwirken/normenausschuesse/nabau/din-spec/wdc-beuth:din21:264066986> (accessed on 1 July 2020).
35. Blocken, B.; Carmeliet, J. On the errors associated with the use of hourly data in wind-driven rain calculations on building facades. *Atmos. Environ.* **2007**, *41*, 2335–2343. [[CrossRef](#)]
36. Steffgen, T. Experimental studies—building physics investigations in condensation water on plaster surfaces. *Pollack Period.* **2019**, *14*, 167–175. [[CrossRef](#)]



© 2020 by the authors. Licensee MDPI, Basel, Switzerland. This article is an open access article distributed under the terms and conditions of the Creative Commons Attribution (CC BY) license (<http://creativecommons.org/licenses/by/4.0/>).